AM1 method rather than the MMFF method, the SS and SR complexes are again very similar.[35,37,38] The $\pi-\pi$ stacking region is found to have a slightly larger separation. When these AM1 structures are used to construct the PPI and PPI-SM models, the resulting interactions are stable. We anticipate that the same change will occur in the ab initio STO-3G calculations[35,37,38] and that the energy decomposition analysis will predict an increase in the relative contribution of the charge-transfer component. Nevertheless, as discussed above, it is not unreasonable to expect that the energy *differences* for the SS and SR model π complexes will not change significantly with increasing accuracy of the calculations. Moreover, we do not consider the sign of the interaction energy for the π complex model to be important because enantiomer separation can be achieved by differences in either attractive or repulsive interactions.

It is conceivable that the model of the SS complex studied herein[12] is incorrect and that, say, other intermolecular interactions are responsible for chiral separation; we are at present investigating this possibility. It should be recalled, however, that the model for the SS complex is in agreement with the experimental studies of Pirkle and Pochapsky.[12] Furthermore, the small separability factors obtained experimentally would suggest that even for a different interaction scheme, a similar analysis would hold; i.e., the SS and SR complexes would have the same primary interactions. Finally we note that formation of dimers of the *R*- and *S*-DNB analytes may compete with the formation of the complexes studied herein.[12] The observed differences in these dimers[12] may need to be considered in order to explain chiral separation and the differences in the observed spectroscopic properties of the complexes.

Conclusions

The model proposed by Pirkle and Pochapsky for the interaction of *S*-NAP with *S*- and *R*-DNB has been studied by molecular mechanics and semiempirical and ab initio quantum chemical methods. The computational studies do find a stable structure for the SS complex which is consistent with the model proposed in terms of the three primary interactions. The computational studies also find a structure for the SR complex in which the same three primary interactions are maintained. Thus enantiomer separation in these systems is not expected to be achieved via a three-point to two-point interaction mechanism but rather by through-space field effects. Such a model has recently been presented for other CSP systems.[2,31] Nevertheless, if a system would be designed in which a three-point versus two-point mechanism were responsible for chiral recognition, then one could expect significantly more efficient separation.

The π functional groups do not appear to provide any differential interactions for the SS versus SR complexes. More consistent with the findings here is that the π interaction contributes equally to the rate at which both enantiomers pass through the CSP. It may, therefore, be unnecessary to incorporate these functional groups into the design of such CSPs and the derivatization of the chiral analytes. Indeed, experimental and computational findings for analogous systems where no π interactions are possible, support this.[19,34,36]

Acknowledgment. We are grateful to K. Lipkowitz for valuable discussions and to one of the reviewers for helpful suggestions.

Registry No. NAP, 103794-11-2; D-DNB, 117096-15-8; L-DNB, 103794-12-3.

(35) Topiol, S.; Sabio, M. Computational Chemical Studies of Chiral Stationary-Phase Models: Complexes of Methyl *N*-(2-naphthyl)alaninate with *N*-(3,5-dinitrobenzoyl)leucine *n*-propylamide. *J. Chromatogr.*, in press.
(36) Hsu, T.-B.; Shah, D. A.; Rogers, L. B. *J. Chromatogr.* **1987**, *391*, 145.
(37) Sabio, M.; Topiol, S. Computational Chemical Studies of Chiral Stationary-Phase Models: The Nature of the Pi Interaction in Complexes of Methyl *N*-(2-naphthyl)alaninate with *N*-(3,5-dinitrobenzoyl)leucine *n*-propylamide. Submitted for publication.
(38) **Note Added in Proof**: Following the submission of this manuscript, we have completed studies which show that the interaction is stable at higher levels of calculation; see ref 35 and 37.

Dimensionality and Metal–Metal and Metal–Oxygen Bonding in the $NaNb_3O_6$ Structure

Maria José Calhorda† and Roald Hoffmann*

Contribution from the Department of Chemistry and Materials Science Center, Cornell University, Ithaca, New York 14853-1301. *Received April 20, 1988*

Abstract: The structures of $NaNb_3O_5F$ and $Ca_{0.75}Nb_3O_6$ were recently described. They contain NbO_3 layers built from NbO_6 distorted octahedra that share edges in one direction and corners in a perpendicular direction. These layers are held together by sodium chains and niobium chains, in which a substantial niobium–niobium bond alternation is observed. Using extended-Hückel band calculations, we explain that the niobium pair formation in the chains is the driving force for the distortions observed elsewhere in the structure. The layers must distort in order to achieve the right environment around the niobiums in the chain. In this process metal–metal bonds are also formed between niobium atoms in the chains and those in the layers, extending over the three-dimensional structure. The influence of electron count on the bonding is also discussed.

Two new niobium ternary oxides, with compositions $NaNb_3O_5F$ and $Ca_{0.75}Nb_3O_6$, were recently synthesized and structurally characterized.[1,2] The two very similar structures contain distorted octahedral Nb_6 units, in which one of the niobium–niobium bonds is extremely short. There are many oxides and halides that contain Nb metal–metal bonding pairs as, for instance, $XNbO_2$ (X = Li,[3] Na[4]), NbO_2,[5] NbI_4.[6] Higher nuclearity clusters are not unusual among niobium halides; consider the Nb_3 triangles in Nb_3I_8,[7] Nb_4 rhombuses in $CsNb_4Cl_{11}$,[8] and Nb_6 octahedra in Nb_6F_{15},[9] to cite but a few examples. On the other hand, such clusters were quite

† Permanent address: Centro de Quimica Estrutural, Instituto Superior Tēcnico, 1096 Lisboa Codex, Portugal.

(1) (a) Köhler, J.; Simon, A. *Angew. Chem., Int. Ed. Engl.* **1986**, *25*, 996. (b) Simon, A., private communication.
(2) Hibble, S. J.; Cheetham, A. K.; Cox, D. E. *Inorg. Chem.* **1987**, *26*, 2389.
(3) Meyer, G.; Hoppe, R. *J. Less Common Met.* **1976**, *46*, 55.
(4) Meyer, G.; Hoppe, R. *Z. Anorg. Allg. Chem.* **1976**, *424*, 128.
(5) Cheetham, A. K.; Rao, C. N. R. *Acta Crystallogr.* **1976**, *B32*, 1579.
(6) Dahl, L. F.; Wampler, D. L. *J. Am. Chem. Soc.* **1962**, *81*, 3150; *Acta Crystallogr.* **1962**, *15*, 903.

0002-7863/88/1510-8376$01.50/0

uncommon in niobium oxides. An exception is the $Mg_3Nb_6O_{11}$ phase,[10] in which the existence of almost regular octahedra of niobium atoms was unequivocally ascertained.[11] The structure of NbO[12] may be described as containing an Nb_6 octahedron with long Nb–Nb bonds.

The presence of metal–metal bonds in some of the above-mentioned materials was further supported by theoretical studies.[13-15]

Niobium–niobium bonds are also known in molecular complexes.[16] Some short bonds are observed in binuclear species, such as $Cs_3Nb_2Cl_9$,[17] $[Nb_2(CO)_2(Cp)_2(C_2R_2)]$[18] (R = CH_3COO), and $Nb_2Cl_6(depe)_2$,[19a] but the shortest appears in $[NEt_4]_2[Nb_2Cl_6(\mu\text{-THT})_3]\cdot CH_3CN$ (THT = tetrahydrothiophene).[19b]

The interesting feature of the two new solids is that not only do they contain a group of six niobium atoms forming a strongly distorted octahedron, but one of the niobium–niobium bonds in it is among the shortest known. The contact distance is 261.4 and 257.8 pm respectively for the Na and the Ca derivatives. While the shortest Nb–Nb bond distance in the binuclear complexes listed above is comparable at 263.2 pm, more typical values are in the range 270–274 pm, ca. 280 pm for many of the solids (NbO_2, Nb_3I_8, Nb_6F_{15}, $Mg_3O_6Nb_{11}$, for instance) and finally 285 pm for metallic niobium.[20]

In the following study, we aim at understanding how the metal–metal bonds are formed and how the whole structure is distorted in order to allow for exactly those short Nb–Nb bonds. In addition, even though the two structures known are almost identical, they occur for different electron counts. The niobium atoms can be assigned different formal oxidation states in each case, as we shall see later. Another aspect to point out is that although we may talk of Nb_6 units, there are no such discrete entities, as they are linked into a three-dimensional network bridged by many oxygen atoms. This explains why we cannot use the Nb_6 octahedra as our reference frame, and a different approach must be tried.

All the calculations are of the extended-Hückel type,[21] using the tight-binding method.[22] Further details are given in the Appendix.

The Structures

Let us start by looking at the structure of $NaNb_3O_5F$,[1] as shown in Figure 1. As the position of the fluorine atoms could not be experimentally determined in the crystallographic study, we shall refer to all light atoms as oxygens. The main features of the structure are chains of niobium atoms (Nb1), chains of sodium atoms, and layers containing niobium (Nb2) and oxygens. While the atoms in the sodium chains are equally spaced, an alternation

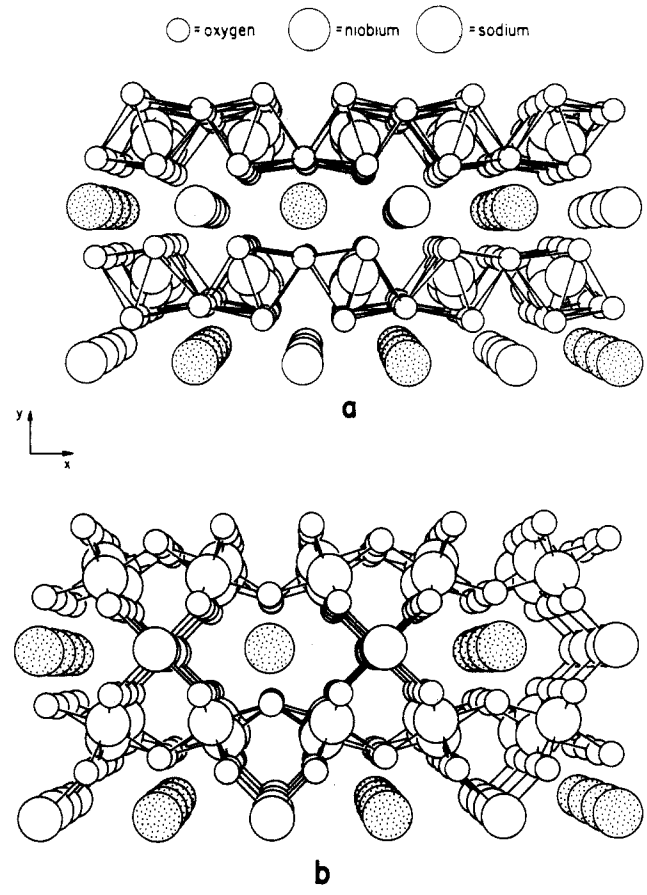

Figure 1. The structure of $NaNb_3O_5F$ seen along z. (a) The coordination polyhedra around Nb2 and the layered structure of the solid are emphasized. (b) The 3D nature of the solid is shown by the Nb–O bonds.

is observed in the Nb1 chains between short (261 pm) and long (388 pm) Nb1–Nb1 bonds. The structural unit of the layers is the $Nb2O_6$ octahedron. These form chains in one direction (along z) by sharing opposite edges and in a perpendicular direction (along x) by sharing vertices and folding. The $Nb2O_6$ units in the layers are severely distorted from an imaginary octahedral starting point. The equatorial plane has a trapezoidal form, **1**, with the metal atom moved away from its center. The O_{ax}–O_{ax} line is not perpendicular to the equatorial plane but tilted, **2**.

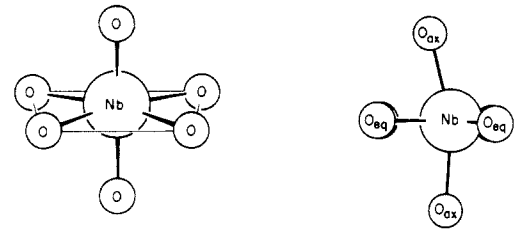

1 **2**

Each of these units shares edges with two others that are rotated 180° around a vertical axis passing through the center, **3**.

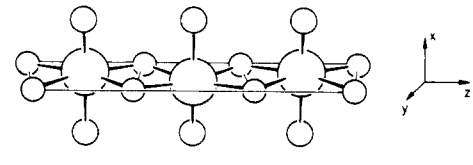

3

As a result, there are two different Nb2–O bonds in the equatorial plane, an alternation of O–O short and long distances along z, and a zigzag chain of Nb2s. The two Nb2–O axial bonds have slightly different lengths. The chains shown in **3** are con-

(7) Simon, A.; von Schnering, H. G. *J. Less Common Met.* **1966**, *11*, 31.
(8) Broll, A.; Simon, A.; von Schnering, H. G.; Schäfer, H. *Z. Anorg. Allg. Chem.* **1969**, *367*, 1.
(9) Schäfer, H.; von Schnering, H. G.; Niehaus, K.-J.; Nieder-Vahrenholz, H. G. *J. Less-Common Met.* **1965**, *9*, 95.
(10) Marinder, B.-O. *Chem. Scr.* **1977**, *11*, 97.
(11) The same Nb_6 units were found recently in $SrNb_8O_{14}$: (a) Köhler, J.; Simon, A.; Hibble, S. J.; Cheetham, A. K., submitted for publication. (b) Simon, A. *Angew. Chem., Int. Ed. Engl.* **1988**, *27*, 159.
(12) Schäfer, H.; von Schnering, H. G. *Angew. Chem.* **1966**, *76*, 833.
(13) Bullett, D. W. *Inorg. Chem.* **1980**, *19*, 1780.
(14) Burdett, J. K.; Hughbanks, T. *Inorg. Chem.* **1985**, *24*, 1741.
(15) Whangbo, M.-H.; Foshee, J. *Inorg. Chem.* **1981**, *20*, 113.
(16) Cotton, F. A.; Walton, R. A. *Multiple Bonds Between Metal Atoms*; John Wiley and Sons: New York, 1980.
(17) Broll, A.; von Schnering, H. G.; Schäfer, H. *J. Less Common Met.* **1970**, *22*, 243.
(18) Gusev, A. I.; Kirilova, N. I.; Struchkov, Yu. T. *Zh. Strukt. Khim.* **1970**, *11*, 54.
(19) (a) Canich, J. A. M.; Cotton, F. A. *Inorg. Chem.* **1987**, *26*, 4236. (b) Cotton, F. A.; Diebold, M. P.; Roth, W. J. *J. Am. Chem. Soc.* **1987**, *109*, 5506.
(20) Greenwood, N. N.; Earnshaw, A. *Chemistry of the Elements*; Pergamon Press: Oxford, 1984.
(21) (a) Hoffmann, R. *J. Chem. Phys.* **1963**, *39*, 1397. (b) Hoffmann, R.; Lipscomb, W. N. *J. Chem. Phys.* **1962**, *36*, 2179, 3489; **1962**, *37*, 2872.
(22) (a) Whangbo, M.-H.; Hoffmann, R. *J. Am. Chem. Soc.* **1978**, *100*, 6093. (b) Whangbo, M.-H.; Hoffmann, R.; Woodward, R. B. *Proc. R. Soc. London*, **1979**, *A366*, 23.

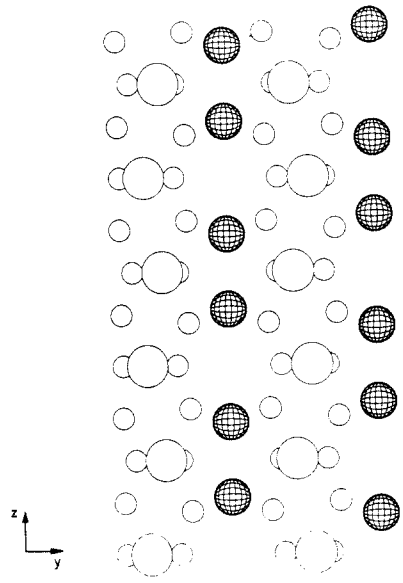

Figure 2. View of $NaNb_3O_5F$ (three unit cells) along x: shaded circles are Nb1, large white circles Nb2, and small white circles oxygen.

nected to similar chains by the axial oxygens (as can be seen clearly in Figure 1) to form layers.

Let us now look at the environment around the Nb1 in the chains. If we consider a Nb1 pair, each of the niobiums is bonded to four oxygens, **4**, which define a nearly perfect square.

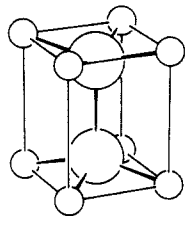

4

The niobiums are moved away from the oxygen squares and toward each other. In Figure 1, we can see that the Nb1 and Na atoms hold the layers together. Indeed, the oxygens that are bonded to each Nb1, **4**, are also part of the Nb2 coordination sphere, and they belong to its equatorial plane (O3). A clearer picture is given by Figure 2 where three unit cells (each containing four $NaNb_3O_5F$ units) are presented, in a view along x. In the middle we can see the Nb1 pairs (shaded) surrounded by oxygens. The long edge of the prism in **4** is also the long edge of the Nb2 octahedron equatorial plane in **1**. The Nb1 pairs are separated by long Nb1–Nb1 bonds. Another feature that emerges from Figure 2 is that the Nb2 are not that far from Nb1, and so **5** represents the coordination sphere of the Nb1 pair in a more realistic way than **4**. The six niobium atoms form a very distorted octahedron, with bridging oxygens.

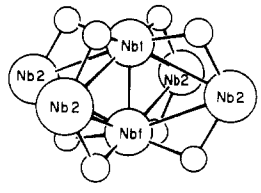

5

The same structure is observed for $Ca_{0.75}Nb_3O_6$, in spite of having two electrons less (per unit cell); the possible existence of $NaNb_3O_6$, with a further two electrons lost but the same structure, has been mentioned.[1b] If we try to derive formal oxidation states for the metal atoms assuming Nb2 to be 4+,[1] then Nb1 will be 2+ or 3+ in the species $Nb_3O_5F^-$ and $Nb_3O_6^-$, respectively, and 2.5+ for the calcium derivative $Nb_3O_6^{1.5-}$.

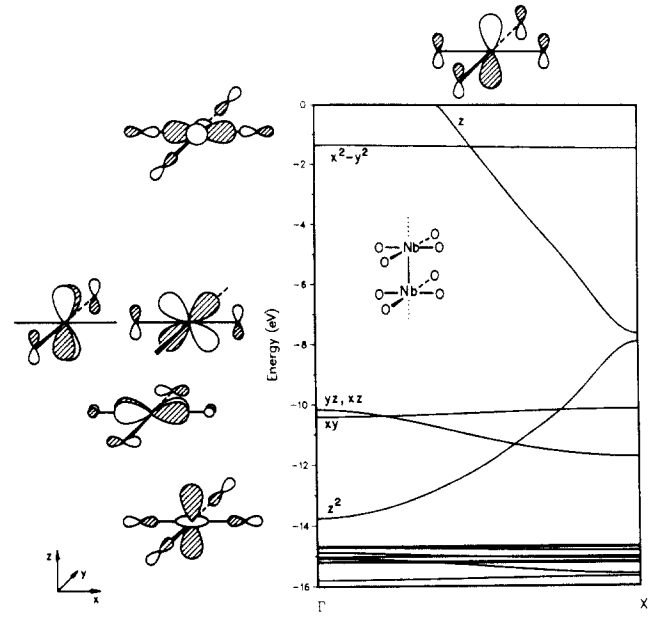

Figure 3. The band structure of the linear chain built from stacked square-planar $NbIO_4$ units. The orbitals of the unit cell at Γ are sketched.

A Model for the Niobium Chains

As the niobium atoms in the chains, Nb1, appear to play a central role in the construction of the whole structure, they provide a good starting point for the analysis. We can consider, as a beginning, that these atoms are only bonded to oxygens, as in **4**. From a different viewpoint, this unit is also a distorted form of the linear chain built by stacking square-planar $NbIO_4$ groups. In this simple model, would a distortion such as moving the niobium atoms toward each other to form a bond be favored for some given electron count?

In order to get an adequate model, let us again look at Figure 2; recall that there is also an alternation of O–O···O bonds along such a distorted chain. What has to be done is move the oxygens in one direction and the niobiums in another, starting from a stack of $NbIO_4$ groups at regular intervals, as shown in **6**.

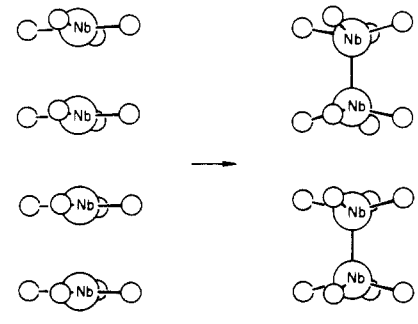

6

In the undistorted chain, the unit cell is the square-planar $NbIO_4$ group and the repeat distance is 325 pm. In a square-planar ligand field, the metal d orbitals will be split into the typical four below one pattern,[23] the higher orbital lying in the square plane and pointing at the ligands. Its energy may be close to that of the metal z orbital, depending on the σ and π donor–acceptor capabilities of the ligands. Since oxygen is a π donor, the Nb z energy is high. All these orbitals are metal–ligand antibonding in character.

Notice that the coordinate system we are using has z along the propagation axis, as in the complete 3D structure. However, x

(23) Albright, T. A.; Burdett, J. K.; Whangbo, M.-H. *Orbital Interactions in Chemistry*; Wiley Interscience: New York, 1985.

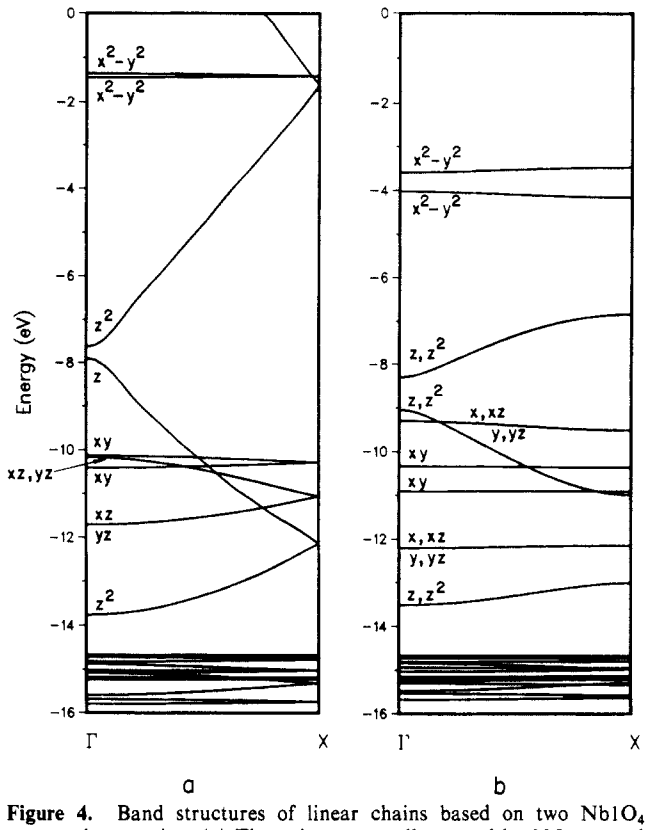

Figure 4. Band structures of linear chains based on two $NbIO_4$ square-planar units. (a) The units are equally spaced by 325 pm, and the unit cell is 650 pm long. (b) Niobiums from the units moved each 32 pm towards each other and oxygens 16 pm in the opposite direction.

and y are directed toward the oxygen ligands, and are thus rotated by 45° relative to x and y in the coordinate system used in describing the complete structure (Figure 1).

The four below one splitting can be seen in the band structure of the undistorted NbIO4, at the zone center (Γ), as shown in Figure 3; $x^2 - y^2$ lies high in energy, much above the other orbitals. The manner in which the bands spread along the Brillouin zone is similar to what happens for other linear chains based on square-planar units, such as the tetracyanoplatinate chain.[22a] Differences will result from having another metal and repeat distance and π donor ligands.

The niobium δ bands, xy and $x^2 - y^2$, are almost flat, as niobium atoms in adjacent unit cells are very far apart (325 pm). Even the π interaction in the xz or yz bands is small, but it will lead to an antibonding crystal orbital at the zone center (Γ) and a bonding one at the edge (X). Only z^2 and z overlap significantly between unit cells, leading to bands with large slopes running in opposite directions as a consequence of their different nodal characteristics.

Lower in energy, we find a bunch of levels, mainly on oxygen. Highest among these are O p-type lone pairs not involved in M–O bonding. Next are orbitals bonding between the metal and oxygens with a stronger contribution from the oxygens. Still lower are the oxygen 2s orbitals, not shown in the figure.

A complete description of the bands for a stack of square-planar units can be found elsewhere,[22a,24,25] so we will not go into more details here.

What will happen to the bands when the distortion referred to in **6** takes place? For that, we must consider a double unit cell, containing two square-planar NbIO4 units; the repeat distance will also be doubled. The same will, of course, apply to the number

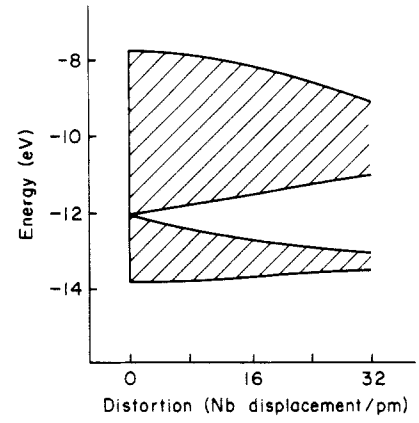

Figure 5. The band width of the z^2 band (shaded) as a function of distortion, measured by displacement of niobium atoms away from the square plane (32 pm is the distorted structure).

of orbitals (or bands) per unit cell. The new representation of the bands is shown in Figure 4a, and, as explained before,[24,25] they can be obtained by "folding back" the bands observed for the single unit cell (note that, as the repeat distance is twice as large, the Brillouin zone is halved). It is important to note that these two representations, those in Figure 3 and Figure 4a, are entirely equivalent.

The bands derived from z^2 and z have the same symmetry inside the zone and they mix. This results in an avoided crossing. Thus the higher half of the z^2 band is labeled z for $k = 0$, while the lower half of the z band is there labeled z^2.

Let us now consider the distortion **6**. The two niobium atoms approach inside the double unit cell, while moving away from niobiums in adjacent units cells (although the oxygens also move, they stay far away from their neighbors along the pairing direction and we do not need to consider their interactions).

As the distortion proceeds we observe that the bands get flatter, they move in energy, and there is a loss of the degeneracies at X. These features are clearly a consequence of the distortion of both the niobiums and oxygens and the lowering of the symmetry. Let us see how this happens.

The gaps that open at X are obviously a result of the lowered translational symmetry, i.e., the pairing distortion. That the bands are flatter also follows from this. In **7** and **8** we show, for instance, the two z^2 basis orbitals that generate the z^2 band of the doubled

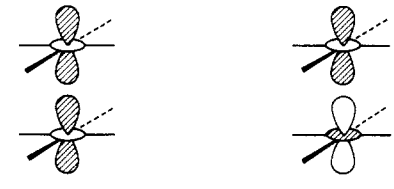

7 **8**

cell. The loss of inversion symmetry at each Nb allows z and z^2 to mix. These orbitals become **9** and **10**.

9 **10**

9 is certainly more localized within the new unit cell, having less overlap with neighboring cells. This would make the band developed from it flat. Even **10**, though it seems to be "pointing" toward the next unit cell, has its inter-unit-cell overlap lowered as a result of this mixing of s, z, and z^2. Similar effects, involving mixing of x, y into xz and yz, lead to a flattening of these bands.

(24) Hoffmann, R. *Angew. Chem.* **1987**, *99*, 871; *Angew. Chem., Int. Ed. Engl.* **1987**, *26*, 846.
(25) Whangbo, M.-H. In *Crystal Chemistry and Properties of Materials with Quasi-One Dimensional Structures*; Rouxel, J., Ed.; Reidel: Dordrecht, 1986; p 27.

Table I. Energy/Unit Cell, Fermi Energy, and Overlap Populations for d^2 and d^3 $Nb1O_4^{x-}$ Linear Chains

	d^2		d^3	
	undistorted	distorted	undistorted	distorted
energy/unit cell (eV)	−1300.51	−1299.64	−1323.34	−1323.95
Fermi level (eV)	−11.58	−12.18	−11.20	−12.14
overlap popln (dist/pm)				
Nb1–Nb1	0.33 (325)	0.80 (261)	0.39 (325)	1.06 (261)
		0.04 (388)		0.03 (388)
Nb1–O	0.55 (197)	0.51 (202)	0.52 (197)	0.48 (202)

A schematic representation of the resulting bands is given in **11**, while in Figure 5 we can see in another way how the z^2 band width varies with pairing.

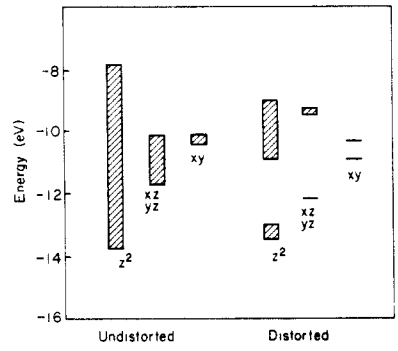

11

If we focus on the important lower z^2 band (recall that most of d block will be unfilled) we see that its center of gravity is stabilized on distortion, but the bottom of the band is actually pushed up at Γ (Figure 4b). The observed behavior is quite different from that of the z^2 band in a $[Pt(NH_3)_4Pt(NH_3)_4Cl_2]^{4+}$ chain with Cl atoms bridging the square-planar units,[15] in which the entire z^2 band is stabilized. The destabilization of the z^2 band at Γ is due to the concurrent oxygen distortion, which cannot be neglected. In **7** the oxygen z contribution is extremely small and the orbital is only weakly σ-antibonding. As the niobiums are pulled out of the plane, the oxygen participation will increase through mixing of strongly π-antibonding Nb z, which is shown in **12**. The resulting orbital should rather be drawn as **13**, instead of **9**.

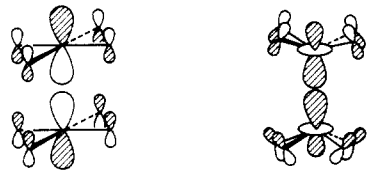

12 **13**

There is now a strong π interaction instead of a weak σ one, which is responsible for the destabilization observed. One can also see this effect in the Crystal Orbital Overlap Population (COOP) curve,[24] which shows a small antibonding peak in the energy range (−13.0 to −13.5 eV) of the lower z^2 band in the distorted chain. No such peak is observed in the corresponding curve for the undistorted chain, in accordance with the almost nonbonding character of that band. The s, z, z^2 band is the only band at those energies.

Will the one-dimensional model polymer distort?

The behavior of the low-energy band z^2 complicates energetic predictions. Referring back to our earlier electron accounting, the Nb1 atoms could be formally Nb^{2+} (d^3) or Nb^{3+} (d^2) in the limiting structures. As there are two niobiums per unit cell in the $Nb1O_4$ chains, three bands will be filled in the first case and two in the other. The energies per unit cell, Fermi level energies, and some overlap populations are collected in Table I.

Although the Nb–Nb overlap population increases strongly and the Fermi level energy drops for either electron count, only for Nb^{2+} (d^3) is there an energy stabilization for the doubled unit cell and thus a preference for a distorted structure. Half-filling of the xz, yz degenerate band in the d^2 case is then not sufficient to overcome the z^2 destabilization near the zone center; rather, the xz, yz band must be completely full, as for d^3.

We cannot forget, however, that this chain is a rather simplified model. In the actual structure, the oxygen atoms are also coordinated to the other niobiums, Nb2, which are, in fact, not very far from Nb1.

We now turn to the two-dimensional slabs containing Nb2.

The Layers

These are made up of $Nb2O_6$ distorted octahedra sharing edges along z (thus becoming NbO_4) and then sharing vertices along x (thus coming to NbO_3). This building-up principle obviously suggests a similar progression for the theoretical analysis.

We begin with the octahedron around Nb2; we saw earlier just how severely distorted that environment is. If we take as the undistorted structure a rectangular bipyramid with slightly shorter $Nb–O_{ax}$ than $Nb–O_{eq}$ bond lengths, it will have to undergo the changes shown in **14**, to get to the right structure.

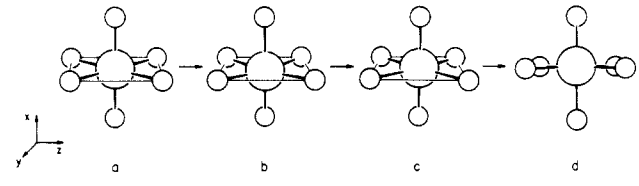

14

In **14a** the four $Nb–O_{eq}$ are equal and $Nb–O_{ax}$ are perpendicular to the equatorial plane. Going to **14b**, we allow the equatorial oxygens to occupy their places in the observed structure, to give alternating O···O pairings in the edge-sharing plane and resulting in two longer $Nb–O_{eq}$ bonds in each octahedral unit. Moving the niobium toward the edge of the trapezoid puts the niobiums in their "real" positions of the whole structure, in a zigzag chain (see **3**), and corrects a little for the disparity between the $Nb–O_{eq}$ bond lengths (**14c**). Finally, the axial oxygens are tilted, **14d** (see **2**).

How much will the bands of the undistorted edge-sharing octahedral $Nb2O_4$ chain be affected by these changes?

The band structure for such an undistorted NbX_4 chain has been described[15,25] and is similar to the one shown in Figure 6 for our undistorted chain **14a**. The nearly octahedral environment is plainly visible: there are low-lying mainly oxygen levels (Nb-O bonding) followed by a large gap and the three "t_{2g}" bands based on Nb2 xz, zy, and $z^2 - y^2$ (they would form the three degenerate levels of t_{2g} symmetry in a regular octahedron), which are Nb–O π antibonding; higher come yz and x^2 ("e_g"), Nb–O σ antibonding.

Note that the coordinate system here is consistent with that of the complete structure. However, a different set of d orbitals is being used to simplify the notation. x^2 is similar to z^2 but oriented along x, while $z^2 - y^2$ looks like $x^2 - y^2$ but points along z and y. Both are linear combinations of z^2 and $x^2 - y^2$ in different proportions.

The niobium atoms in adjacent cells are 325 pm apart, so their interaction is small. Interactions between unit cells occur through the bridging oxygens. In the "t_{2g}" bands the oxygen and niobium orbitals overlap weakly, mostly in a π-type way so the dispersion is small. In the other bands, the oxygen lone pairs have better

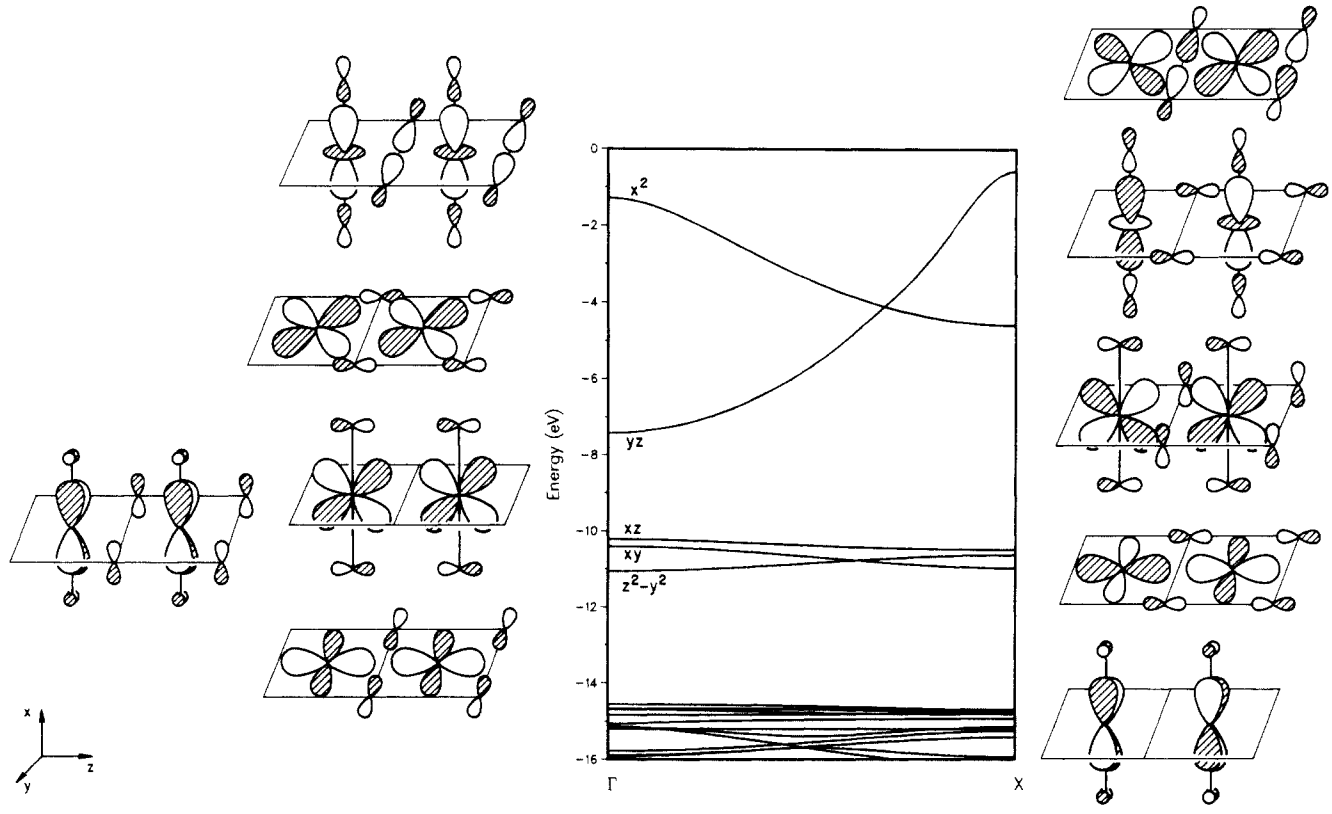

Figure 6. Band structure of the linear chain built from $Nb2O_6$ distorted octahedral units (see text) sharing opposite edges. The orbitals for two adjacent unit cells are sketched at the center and edge of the Brillouin zone.

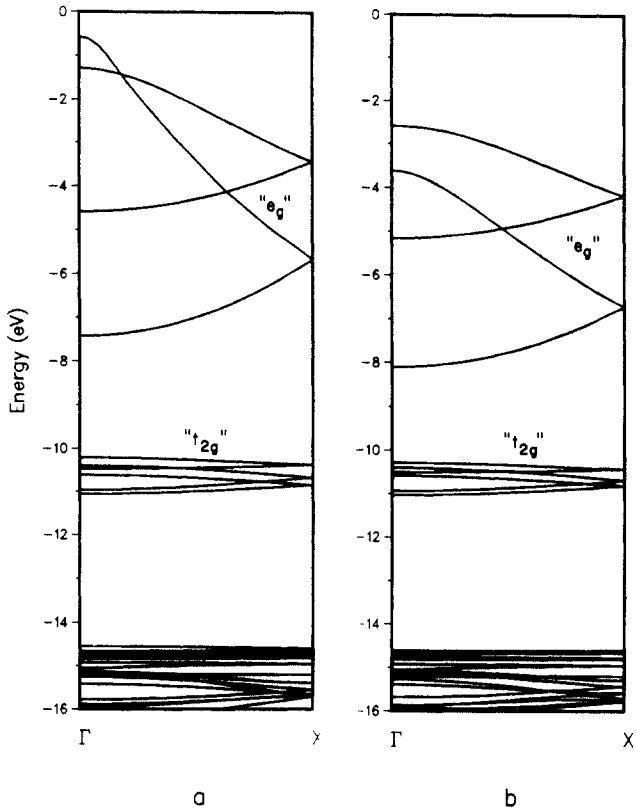

Figure 7. Band structures of linear chains based on two edge-sharing $Nb2O_4$ units. (a) The basic motif is as shown in **14a**. (b) Each unit is distorted as in **14d**.

overlap with niobium yz and x^2, allowing the antibonding character of the bands to change very much along the Brillouin zone.

In order to distort the chain as shown in **14a,b,c,d** we start by doubling the unit cell, thus folding back the bands (Figure 7a). Distortion from **14a** to **14b** removes the vertical xz symmetry plane

Table II. Energy/Unit Cell, Fermi Energy, and Overlap Populations for the Distorted $Nb2O_4$ Chain

	undistorted **14a**	distorted **14d**
energy/unit cell (eV)	−1277.76	−1276.49
Fermi energy (eV)	−10.94	−10.93
overlap popln (dist/pm)		
Nb2–Nb2	−0.015 (325)	−0.028 (331)
$Nb2–O_{eq}$	0.41 (205)	0.33 (215)
		0.48 (201)

but a screw axis takes its place, **15**, and is kept throughout the distortion: thus the degeneracies at the zone edge are retained.

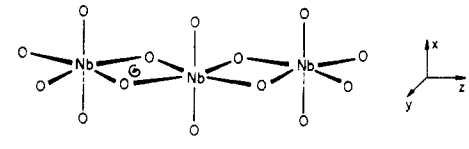

15

The band structure for the distorted chain (**14d**) is shown in Figure 7b. The lowering of symmetry has allowed bands to mix but no spectacular changes occurred. The "e_g" bands are stabilized, due to poorer overlap between oxygen and niobium orbitals, which makes them less antibonding. The "t_{2g}" bands remain almost the same. As the metal–ligand interaction is weaker, they are not so sensitive to the metal–ligand orientation.

Very importantly, in these band structures there is a large gap between the metal and oxygen levels (−11.0 to −14.5 eV). This is the region of energy where we found three of the d bands for the distorted square-planar $Nb1O_4$ chain (the Nb–Nb bonding bands, Figure 4b), showing how differently the metal d orbitals are affected by a square-planar or an octahedral ligand field. The result is important in that it allows us to look for different types of bonds as a function of energy, instead of having only one bunch of levels.

We can compare the energy per unit cell, Fermi level, and some overlap populations for our undistorted and distorted $Nb2O_4$ chains, as shown in Table II.

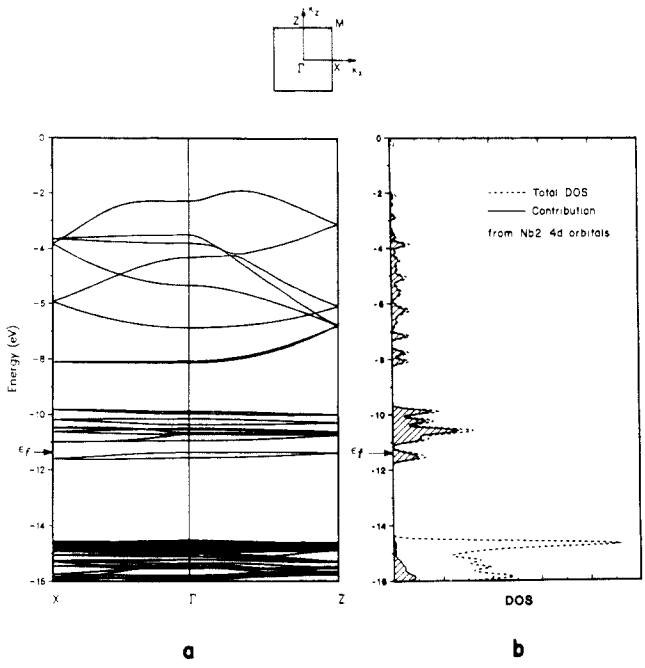

Figure 8. (a) Band structure for a $Nb2O_3$ layer containing octahedral $Nb2O_6$ distorted octahedra sharing vertices and edges (as in **16**) shown along two symmetry lines of the two-dimensional Brillouin zone. (b) The total density of states (- - -) and a projection of the Nb2 4d states (dark area) for the same layer.

The overlap populations were calculated for Nb^{4+} (d^1), but they should not be much changed for higher electron counts, as the bands that are being filled are the almost nonbonding "t_{2g}". On the average, they are not very different for the distorted structure. The Fermi level is the same, because as we saw before, the lower d-bands remain mostly unchanged. Only the energy per unit cell is increased, which is not surprising. As the Nb–O antibonding "e_g" bands are stabilized, their bonding, occupied, counterparts should be destabilized. This means that this distortion is not a stabilizing one, contrary to the pairing distortion observed for the edge-sharing octahedral NbX_4 chain.[15] We can tentatively conclude that it is adopted in order to achieve a suitable geometry for the oxygens to coordinate the Nb1 in the chains.

However, before jumping to these conclusions, we should see what happens for the complete layer, and not only one chain. We must add another dimension.

Along x the infinite, edge-sharing $Nb2O_4$ chains share vertices, and also fold to achieve the final slab geometry. We did study the effect of vertex sharing alone, but it is minor, and so it is best to proceed to the final two-dimensional slab of **16**. Its band structure is shown in Figure 8a. The $\Gamma \rightarrow Z$ line in this band structure can be compared with Figure 7b, keeping in mind that the unit cell has been doubled.

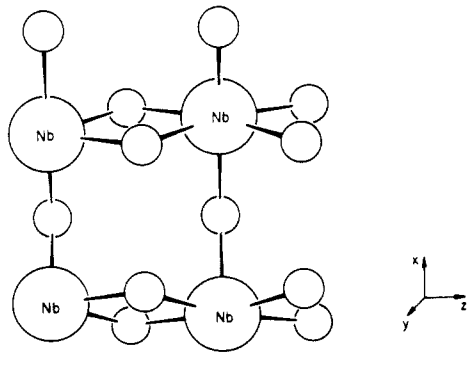

16

In Figure 8b, we can see the total density of states (DOS)[24] for this layer, along with a projection of the Nb2 4d orbitals. We still have the same band pattern as before (three main groups separated by large gaps: the Nb2–O bonding levels, the "t_{2g}" and "e_g" sets). Each of the layers in the solid is far from its neighbors, and their interaction is small. They are held together by the Nb1 and Na chains. If interaction of Nb2 and O3 (oxygens in the equatorial planes) with Nb1 occurs, we expect to see some shift in their projected density of states when we compare them with those from the three-dimensional solid.

This distorted layer is, once again, energetically unfavored compared to an orthogonal (not folded) layer built from the $Nb2O_6$ unit in the same way (edge sharing in one direction and corner sharing in the other). A further comparison between distorted and undistorted structures is of limited value, because such a layer would not have the right geometry to interact with the other (Nb1) metallic chain. If this were not the case, the layer might well distort in a different way, as seen in similar NbO_2 layers. In this particular compound a Nb–Nb pairing along the edge-sharing direction is observed, while the alternation Nb–O···Nb occurs in the other direction. The resulting electronic structure of the solid, NbO_2, is in accordance with its semiconducting properties.[26]

The Complete Structure

The three-dimensional structure is body-centered orthorhombic, space group *Immm*, with $b > a > c$. In each primitive unit cell there are two Nb_3O_6 units (with two Nb1 and four Nb2 atoms). The Nb1 pairing occurs along z, so we want to look at the bands in the corresponding line of the Brillouin Zone (k_z) in order to compare them with those in the one-dimensional $Nb1O_4$ chain.

In Figure 9 are plotted the bands for the three directions k_x, k_y, and k_z or $\Gamma \rightarrow \Sigma$, $\Gamma \rightarrow X$, $\Gamma \rightarrow \Lambda$, several gaps being observed in each plot. However, we should look at the total density of states plot (which was calculated by averaging over the whole zone) to be sure of the existence of gaps (Figure 10, dashed line). The first large gap occurs around −14.5 eV and separates the Nb–O bonding levels from the first group of mainly d bands. These particular d bands fall in the same region as the lower d bands of Nb1 in a square-planar field of oxygens in the model Nb1O4 chain. After the next gap comes what we may call the "t_{2g}" levels of Nb2 in the layers (between −12.0 and −9.0 eV with an eventual gap at −11.3 eV), and, finally, the Nb2 "e_g" bands, higher in energy. We have to look at some decompositions of densities of states to confirm these simplified assumptions. In Figure 10, the total density of states is shown by the dashed line; the contribution of Nb1 4d orbitals is the dark area of Figure 10a. Notice the importance of their contribution to the block of levels between −12.8 and −14.0 eV. Nb2 4d orbital contributions are shown in Figure 10b (dark area) and they also contribute most of the total DOS between −9.0 and −12.0 eV, as well as to higher energy bands. However, both Nb1 and Nb2 have states throughout the energy window, which suggests an interaction between them. We shall return to this point later.

The Fermi level is shown for $Nb1^{3+}$ (d^2) and $Nb2^{4+}$ (d^1), which leads to four filled d bands (Figure 9). This corresponds to occupying all the bands below the small gap around −11.3 eV. The material $NaNb_3O_6$ should be a semiconductor.

Before looking at this band structure in more detail, let us imagine which undistorted three-dimensional structure we could use to compare with the real one. We may, for instance, introduce the $Nb1O_4$ undistorted linear chain (with square-planar $Nb1O_4$ units) in the whole structure. For that, we have to "undistort" the Nb2 and the O3 (oxygens in the equatorial plane around Nb2). All the Nb1–Nb1 bond lengths, as well as the O3–O3 bond lengths, will be 325 pm, along z. In a view like the one shown in Figure 2, we would no longer see the bond alternation. The equatorial plane in the $Nb2O_6$ octahedron is a rectangle, but we keep the Nb2 atom away from the center. In this model, the Nb1 atoms will still hold the layers together through their interaction with O3 oxygens, but the Nb1–Nb1 bonds will be lost, as the

(26) Whangbo, M.-H. *Inorg. Chem.* **1982**, *21*, 1721.

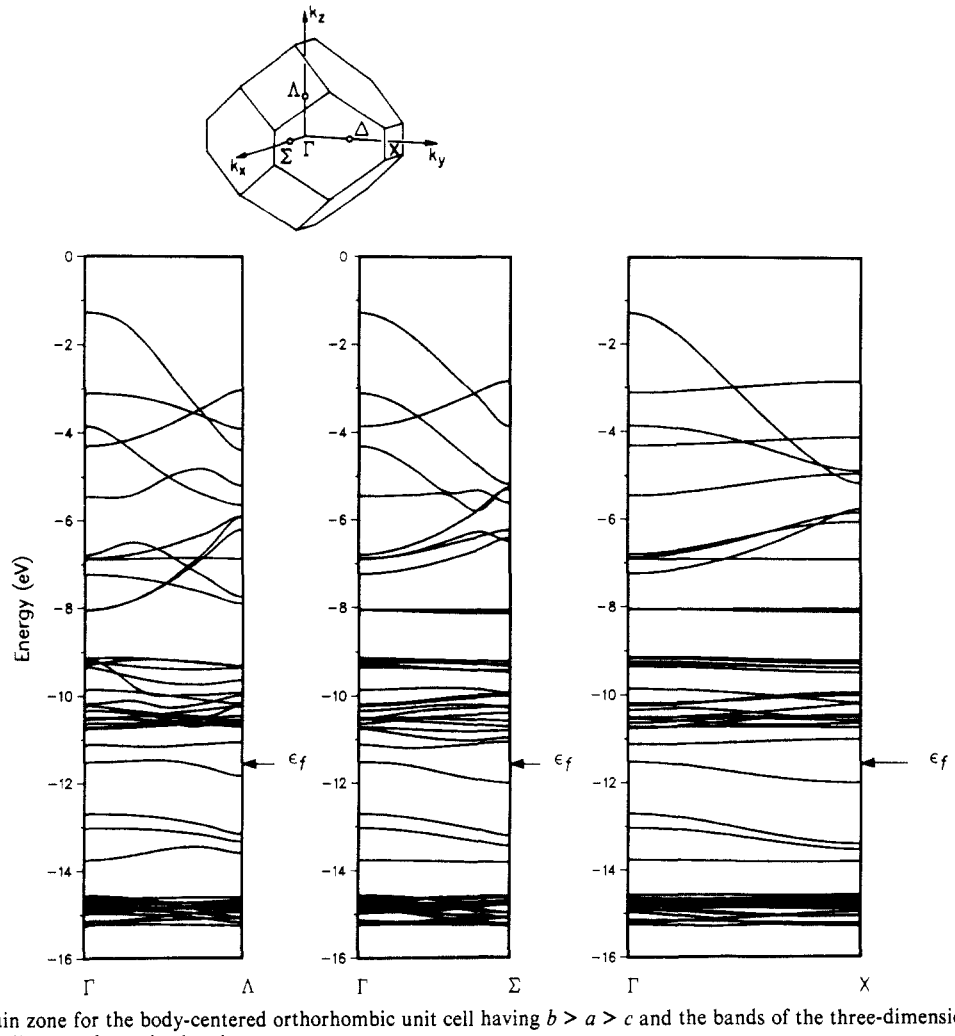

Figure 9. The Brillouin zone for the body-centered orthorhombic unit cell having $b > a > c$ and the bands of the three-dimensional structure plotted along three symmetry lines as shown in the plots.

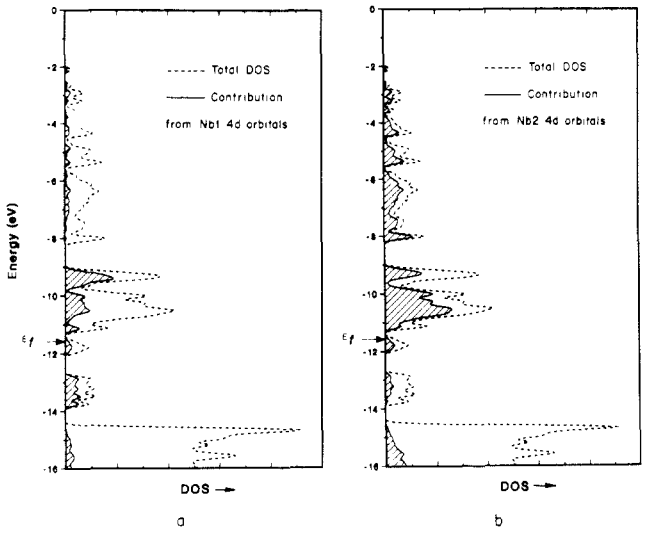

Figure 10. Total density of states (---) and projected (dark area) niobium 4d states in the three-dimensional structure: (a) Nb1 atoms (b) Nb2 atoms.

niobiums are far from one another.

The undistorted structure, whose bands we do not show here, is less stable than the observed one. A comparison is made in Table III.

Qualitatively, these results compare well with those in the one-dimensional chain (Table I). Let us add that these calculations assumed d^2 Nb1 and d^1 Nb2. The main difference here is a

Table III. Energy/Unit Cell, Fermi Level Energy, and Overlap Populations for "Undistorted" $Nb_3O_6^-$ and the Real Structure for d^2 Nb1 and d^1 Nb2

	undistorted	distorted
energy/unit cell (eV)	−4032.67	−4033.24
Fermi energy (eV)	−11.16	−11.56
overlap popln (dist/pm)		
Nb1–Nb1	0.31 (325)	0.70 (261)
Nb1–O3	0.47 (197)	0.44 (202)
Nb1–Nb2	0.09 (324.5)	0.15 (309)

stabilization of the distorted structure for d^2 Nb1. Also, we have now a Nb1–Nb2 overlap population, which did not appear before, as Nb2 were not included in our primitive model chains.

From what has been said, we can infer that the distorted structure is energetically favored due to the formation of strong Nb1–Nb1 bonds in the pairing process (from comparing to the $Nb1O_4$ chain), this effect being stronger than the destabilization we found for the distortion of the two-dimensional layers built up from $Nb2O_6$ octahedra.

Another factor that is important in favoring this structure is the formation of Nb1–Nb2 bonds as suggested by the overlap population. Another look at Figure 1 reveals that the movement of the Nb2 atoms toward one edge of the equatorial plane in their octahedral environment leads to the formation of a zigzag chain and an approach to the nearest Nb1 pair, **17**.

Let us now look at the bands in more detail, in order to find evidence for these Nb1–Nb1 and Nb1–Nb2 bonds.

The three lower d bands in Figure 9, lying between −12.5 and −14.0 eV, remind us of the corresponding bands in Figure 4b for the linear chain. As we saw in the DOS plots (Figure 10b) they

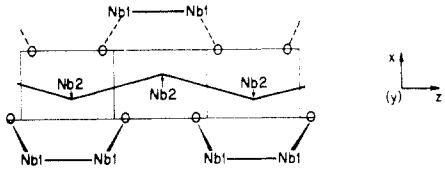

17

are mainly located on the Nb1 atoms (there are twice as many Nb2 for unit cell as Nb1). The contribution of the Nb1 atoms to the crystal orbitals at Γ is represented in **18** (band at −13.76 eV), **19** (band at −13.03 eV), and **20** (band at −12.70 eV).

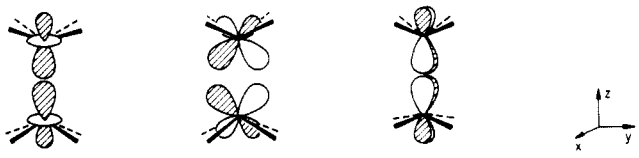

z^2, z yz, y xz, x

18 **19** **20**

These orbitals are very similar to those shown before for the model $Nb1O_4$ chain. These orbitals are strongly Nb1–Nb1 bonding, which agrees with the COOP curve shown in Figure 11. We find, indeed, only bonding peaks in the energy range of those three bands (−12.7 to −14.0 eV).

The fourth lowest d band in Figure 9, starting at −11.52 eV at Γ, still has a strong contribution from Nb1 (40% per NbO_6 unit) but is only slightly bonding between the pair of Nb1 atoms, as z and z^2 mix in such a way as to decrease the overlap between orbitals on those atoms. It is just the opposite of what happens in **18**. Other smaller contributions to this band at Γ come from Nb1 $x^2 - y^2$ and will give rise to a weak δ interaction. The COOP curves in Figure 11 show that this band is slightly bonding between Nb1 atoms, and bonding between Nb1 and Nb2 (Nb2 atoms account for 20% of the crystal orbital at Γ, through z^2 and xy). This band is occupied for all electron counts.

The next d band (−11.11 eV) is the one whose occupation will change with increasing electron count. Nb1 atoms only contribute 28% to the crystal orbital at Γ, mainly through $x^2 - y^2$, as in the previous band, while Nb2 participate with 20% through $x^2 - y^2$ and z^2. The COOP curves in Figure 11 show this band to be Nb1–Nb1 nonbonding, but Nb1–Nb2 bonding.

Another interesting observation is that all three lower d bands are stabilized relative to the corresponding bands in the linear model chain, although not by a great deal. As the oxygens occupy the same positions in the structure as in the model, a possible explanation could implicate a bonding stabilizing interaction with other nearby atoms, namely Nb2.

An indication that it is indeed so is given by the other COOP curves in Figure 11, where the character of the bands relative to Nb1–Nb2 and Nb1–O3 bonds averaged over the Brillouin zone is shown. This group of three bonds with energies between −12.7 and −14.0 eV is indeed bonding between Nb1 and Nb2, as we predicted, and antibonding between Nb1 and O3.

Still another indication of Nb1–Nb2 bonding comes from examining contributions of individual d orbitals on the metals to the total DOS. We find resonances, indicative of mixing, therefore interaction between certain groups of levels: Nb2 $x^2 - y^2$ and z^2 with Nb1 xz (in the highest band, **20**); Nb2 xy with Nb1 yz (in the middle band, **19**); Nb2 xy and z^2 with Nb1 z^2 (in the lower band, **18**), although in a smaller degree.

All these results point to the existence of Nb1–Nb1 and Nb1–Nb2 bonds in the structure, which build the distorted octahedral unit Nb_6. The formation of the strong Nb1–Nb1 bonds seems to be the driving force for the distortion observed in the 3D structure. The weaker Nb1–Nb2 bonds also formed (as shown by the increase in overlap population in Table III) also contribute to a stabilization of the distorted structure. However, all the niobiums are under the influence of the strong oxygen crystal field.

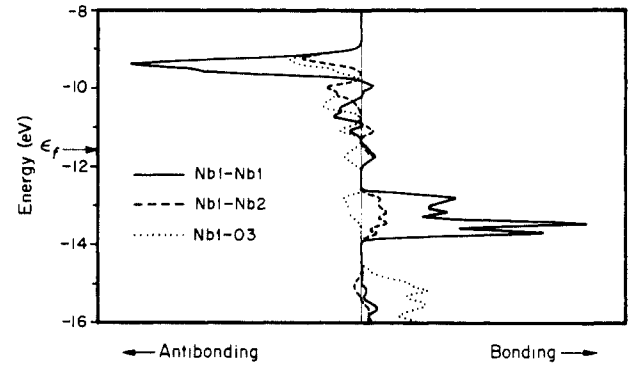

Figure 11. Crystal orbital overlap population (COOP) curve for the Nb1–Nb1 short bond (—), Nb1—O3 (···), and Nb1—Nb2 (- - -) bonds in the Nb_3O_6 structure, showing the bonding or antibonding character of the bands across the energy window.

Table IV. Overlap Populations and Charges for $Nb_3O_6^{x-}$

	$Nb_3O_6^-$	$Nb_3O_6^{1.5-}$	$Nb_3O_5F^-$
d electrons/2 formula units	8	9	10
overlap popln			
Nb1–Nb1	0.70	0.70	0.70
	0.03	0.09	0.15
Nb1–O3	0.44	0.43	0.42
Nb1–Nb2	0.15	0.16	0.16
charges			
Nb1	0.70	0.48	0.27
Nb2	1.71	1.61	1.51
O1	−0.99	−0.99	−1.00
O2	−1.01	−1.02	−1.02
O3	−0.78	−0.80	−0.81

Different Electron Counts and Discussion

The structure studied in this paper is observed for more than one electron count with minimal structural changes. We may wonder if this agrees with the type of bonding we have been describing. For that, we can compare the overlap populations of the more important bonds for three electron counts. The results are given in Table IV.

The Nb1–Nb1 overlap population remains unchanged, as the bands responsible for this bond are all three filled in each case, leading to what we may call a triple bond between the niobium atoms (with one σ and two π components). The COOP curve (Figure 11) shows only small peaks around the Fermi level energy. For the Nb1–Nb2 bond we observe (Figure 11) that, as the Fermi level is moved from −11.56 to −11.04 eV, bands that are bonding will be filled, and a slight increase in overlap population occurs. The same is happening for the long Nb1–Nb1 bond in the chains; bonding levels are occupied and the bond strengthens. On the other hand, we see in Figure 11 that these same levels are also metal–oxygen antibonding, which accounts for the small decrease in overlap population shown for the Nb1–O3 bond.

On the whole, the changes are not very large as we vary the electron count, so we should expect the bond lengths to be nearly the same. This is true for Nb–Nb bonds (260, 258, 261 pm for Nb1–Nb1; 308, 306, 309 pm for Nb1–Nb2). Nb1–O bonds (201, 196, 202 pm, respectively) show greater differences, but the oxygens in the $Ca_{0.75}Nb_3O_6$ structure could not be very accurately determined, so the 196 pm bond length may, in fact, be longer.

Let us look at the charges. Although both niobiums are positively charged, the Nb2 atoms carry a much larger charge. This agrees with our assignment of a higher formal oxidation state to them. Also, as electrons are added, they move essentially onto the Nb1 atoms, the charge of these metal centers decreasing accordingly. The oxygens are mostly left unchanged; among them, the more negatively charged are the axial oxygens, O1 and O2. The fluorines, which could not be located in the structure of $NaNb_3O_5F$ (but whose presence was ascertained by analytical means[1]), should occupy one of these axial positions, being very

Table V. Parameters Used in the Extended-Hückel Calculations

atom	orbital	H_{ii}/eV	ζ_1	ζ_2	C_1[a]	C_2[a]
Nb	5s	-10.10	1.89			
	5p	-6.86	1.85			
	4d	-12.10	4.08	1.64	0.6401	0.5516
O	2s	-32.30	2.275			
	2p	-14.80	2.275			

[a] Coefficients used in the double-ζ expansion of the 4d orbitals.

electronegative atoms.[27] The other advantage of this position is that they would not interfere with the bonding about Nb1. It is unlikely that the highly symmetrical coordination of this metal will incorporate a strange atom.

Do we have a triple bond between the paired Nb1's in this structure, as it has been described? First let us look at some of the bond length systematics. In the complex $[NEt_4]_2[Nb_2Cl_6(\mu\text{-}THT)_3]\cdot CH_3CN$ the metal–metal bond length is 263.2 pm. The bonding between the two formally Nb^{2+}, d^3, has been described as being a triple bond.[19b] Still slightly shorter Nb–Nb bonds are found in the tetramers $[Na(THF)_3]_2[Nb_2X_5(THT)_3]_2$, respectively 261.0 pm for X = Cl and 260.7 pm for X = Br, each unit containing two Nb–Nb triple bonds separated by a long Nb···Nb distance.[19b] In the molecular complexes $Cs_3Nb_2Cl_9$,[17] $[Nb_2(CO)_2(Cp)_2(C_2R_2]$,[18] and $Nb_2Cl_6(depe)$,[19a] the niobium–niobium bond lengths are in the range 270–274 pm. They are thought to be double bonds as the two metals are formally Nb^{3+}, d^2. The longer bonds in the solids are closer to being single bonds.

If we examine the orbitals of our delocalized three-dimensional structure, we find that three of the four bands occupied are primarily localized on Nb1. Furthermore they have the shape of **18**, **19**, and **20**. While there is some admixture of other orbitals, it is clear that these levels describe a set of $\sigma + 2\pi$ bonds. So a triple bond description is quite appropriate.

Acknowledgment. M.J.C. is grateful to the Calouste Gulbenkian Foundation for its support of her stay at Cornell. M.J.C. also thanks Marja Zonnevylle and Jing Li for sharing their expertise and for helpful discussions. Our work was supported by the National Science Foundation, Grant DMR 821722. We thank Jane Jorgensen and Elisabeth Fields for the drawings and Joyce Barrows for the production of this manuscript.

Appendix

All the calculations were of the extended-Hückel type,[21] with the tight-binding approach.[22] The parameters are collected in Table V.

The geometry of $NaNb_3O_5F$[1] was used for the three-dimensional structure and simpler models taken from it, as described in the text.

The *k*-point sets were chosen according to the geometrical method of Ramirez and Böhm.[28]

Registry No. $NaNb_3O_6$, 117067-24-0; $NaNb_3O_5F$, 104848-57-9; $Ca_{0.75}Nb_3O_6$, 109011-02-1; Nb, 7440-03-1.

(27) Burdett, J. K. *Acc. Chem. Res.* **1982**, *15*, 34.

(28) Ramirez, R.; Böhm, M. C. *Int. J. Quantum Chem.* **1986**, *30*, 391.

A New Technique To Calculate Low-Energy Conformations of Cyclic Molecules Utilizing the Ellipsoid Algorithm and Molecular Dynamics: Application to 18-Crown-6

Martin Billeter,[†] Allison E. Howard, Irwin D. Kuntz, and Peter A. Kollman*

Contribution from the Department of Pharmaceutical Chemistry, University of California—San Francisco, San Francisco, California 94143. *Received August 17, 1987*

Abstract: We present a new approach of generating low-energy conformations of cyclic molecules. It combines a constrained optimization method known as the ellipsoid algorithm for efficient sampling of sterically allowed conformations and molecular dynamics simulations for local exploration of the conformation space around the structures obtained with the ellipsoid algorithm. The methods are applied to the ionophore 18-crown-6. It is shown that this approach can find the conformations obtained in earlier theoretical and experimental investigations, as well as locate new low-energy conformations which have not been previously studied. The energy evaluation of the conformers obtained by the ellipsoid algorithm was carried out using the AMBER molecular mechanics force field. We provide preliminary data which indicate, contrary to current practice, it may not always be appropriate to scale the 1–4 electrostatic interactions when using this force field.

Computational chemistry has profited greatly by the increased size and speed of computers in recent years. Chemists now routinely perform ab initio level calculations[1] on a wide variety of molecules. Larger molecules, including proteins, are being studied by increasingly complex computational methods,[2] including molecular mechanics and dynamics. However, researchers using such methods are hampered by the number of local minima in complex molecules. To avoid the danger of becoming trapped in local minima, one often selects "good" starting structures; this can, however, lead to a biased result. The problem of local minima is especially acute for cyclic molecules since, owing to the interdependence of torsion angles,[3] it is not trivial to obtain an unbiased sampling of closed-ring structures.

Feasible starting structures for energy refinement methods can be generated for acyclic molecules by dihedral grid searches,[3d] but the extension of these searches to cyclic systems is more difficult and such a method quickly expands beyond the realm of practicality as the size of the system increases. Graphics modeling, while rapid, suffers both from bias and the difficulty

[†] Current address: Institut für Molekularbiologie und Biophysik, Eidgenössische Technische Hochschule—Hönggerberg, CH-8093 Zürich, Switzerland.

(1) Hehre, W. J.; Radom, L.; Schleyer, P. v. R.; Pople, J. A. *Ab Initio Molecular Orbital Theory*; Wiley-Interscience: New York, 1986.

(2) Seibel, G.; Kollman, P.; Weiner, S.; Singh, U. C. *Telematics Informatics* **1985**, *2*, 307–310.

(3) (a) Go, N.; Scheraga, H. A. *Macromolecules* **1970**, *3*, 178–187. (b) Go, N.; Scheraga, H. A. *Macromolecules* **1973**, *6*, 273–281. (c) Dygert, M.; Go, N.; Scheraga, H. A. *Macromolecules* **1975**, *8*, 750–761. (d) Motoc, I.; Dammkoehler, R. A.; Marshall, G. R. In *Mathematics and Computational Concepts in Chemistry*; Trinajstic, N., Ed.; Ellis Horword: Chichester, England, 1986; pp 222–251.

0002-7863/88/1510-8385$01.50/0